NASA-CR-196861

OCT
22738
P. 33

Grant # NAG-1-1402

Entitled

"Vortex Mixing In Compressible Flow"

Laser Doppler Velocimeter Measurements of Boundary Layer Velocity and Turbulent Intensities in MACH 2.5 Flow

Final Report

Submitted to:
Nasa Langley Research Center

Jesse Sewell , *Graduate Student*
Dr. Larry Chew, *Assistant Professor*

University of Central Florida
Department of Mechanical and Aerospace Engineering
Orlando, Florida 32826

N95-11709
Unclas
G3/34 0022738

(NASA-CR-196861) LASER DOPPLER VELOCIMETER MEASUREMENTS OF BOUNDARY LAYER VELOCITY AND TURBULENT INTENSITIES IN MACH 2.5 FLOW Final Report (University of Central Florida) 33 p

Introduction

In recent years, the interest in developing a high-speed civil transport has increased.[1] This has led to an increase in research activity on compressible supersonic flows, in particular the boundary layer. The structure of subsonic boundary layers has been extensively documented using conditional sampling techniques which exploit the knowledge of both u and v velocities.[2] Researchers using these techniques have been able to explore some of the complex three-dimensional motions which are responsible for Reynolds stress production and transport in the boundary layer. As interest in turbulent structure has grown to include supersonic flows, a need for simultaneous multicomponent velocity measurements in these flows has developed. The success of conditional analysis in determining the characteristics of coherent motions and structures in the boundary layer relies on accurate, simultaneous measurement of two instantaneous velocity components.

Supersonic Boundary Layers

Experimental fluid mechanics has for many years, made use of mechanical measuring probes to obtain information on fluid velocity. Total pressure probes, in conjunction with static pressure probes, have provided the principle means of measuring mean velocity. Hot-wire or hot-film anemometers have been the principle means of measuring instantaneous velocity. From the instantaneous velocity, the root mean square (rms) velocities and velocity correlations can be calculated. Laser Doppler Velocimetry is an optical technique that allows the measurement of local, instantaneous velocity of tracer particles suspended in the flow. The most common

methods used to date for measuring the boundary layers of supersonic flows are Hot-wire or Hot-film anemometry and Laser Doppler Velocimetry.

Laser Doppler Velocimetry

It is important to note that LDV measures the absolute velocity of particles in the flow and not the flow itself. LDV techniques do not depend on temperature, pressure or other flow parameters. Seed particles are injected into the flow to "trace" it and scatter the incoming laser light. These particles must not only track the flow accurately, but must also be present in sufficient number throughout the flow field to allow complete, reliable data acquisition.[3] In addition, LDV is an optical technique that does not disturb the flow and the velocity is not measured behind a shock wave or any other type of obstruction. This makes the technique particularly suited for measurements in flow reversals and recirculations or environments where mechanical probes are not well suited.

LDV has been successfully applied in subsonic and transonic flows; however, as soon as the flow becomes supersonic, difficulties arise.[4] Some of these difficulties include: signal processor limitations due to high frequencies associated with high speed flows; extremely high velocity gradients within the measurement volume; finding a suitable seed particle that will properly follow the flow and a few seconds or minutes of "blow down" duration in a wind tunnel. A short blow down duration means only a few runs per day, which inhibits the detailed study of LDV systems in high speed flows.

Research Objectives

The objective of this research is to develop a methodology to examine supersonic flow boundary layers using an LDV. Since each LDV application involves a flow seeder, it is necessary to develop a flow seeding apparatus. For high speed flows, the seed particles must be monodisperse and submicron in size.[3] In this study we will develop a seeder that utilizes the moisture in the air to produce a stream of uniform sized particles which are well suited for high speed LDV applications.

In a supersonic boundary layer, the streamwise velocity is much larger than the transverse velocity component. This creates difficulty in obtaining simultaneous two dimensional velocity measurements in the boundary layer. We will solve this problem by using a new frequency shifting technique. To the best of our knowledge this technique has not been published in literature.

This study will provide additional information for the application of experimental LDV techniques in high speed flow boundary layers. In addition, it also provides complete analysis over a broad spectrum of turbulence data needed for a data base to be used for computational fluid dynamics (CFD) code verification.

Literature Review

Current State of Boundary Layer Research

It is important to measure the characteristics of supersonic boundary layer flows for the following reasons: 1) Boundary layer and shockwave interaction, the interaction between shockwaves and the turbulent boundary layer is an important problem in modern fluid dynamics.

Many practical applications in high speed aerodynamics and propulsion evidence the phenomenon and understanding these interactions is relevant and important.[5] 2) The transition from laminar to turbulent in the boundary layer, the ability to experimentally determine where boundary layer transition occurs over a test configuration is important for many reasons. For example, to compare computational drag predictions with wind tunnel values, it is necessary to know where transition actually occurs on the wind tunnel model.[6] Also for high angle of attack research, knowing whether the boundary layer is laminar or turbulent on the forebody of a configuration will determine whether or not the data will have to be corrected before being applied to full scale flight.[6] 3) Prediction and control of transition in high speed flows, transition from laminar flow to turbulent flow in supersonic and hypersonic boundary layers has important ramifications for the supersonic laminar flow control. The applications are directly related to the design of the National AeroSpace Plane (NASP). The exact location of transition is crucial for proper aero/thermal design. Currently no prediction capabilities exist for location of transition in the boundary layer of hypersonic flows.[1] The experimental analysis of boundary layers is essential to verify CFD codes that attempt to predict such transition points.

The non-intrusive nature of LDV makes the method well suited for velocity measurements in regions where probes or hot-wire techniques simply cannot be used. DeCampos and Falcao[7] (1993) used an LDV to perform three dimensional measurements on tip vortices in cavitating and non-cavitating conditions in the tip region of compressor blades. They were able to measure the tip vortex flow field in the near wake of an elliptical foil. The effects of different Reynolds numbers in non-cavitating and cavitating flow fields were compared. Atomized mineral oil was used as seed particles due to the abrasive nature of metal-oxide particles.

Romano (1992) performed velocity measurements in flow regions of high turbulence intensity in the wake of a delta wing using LDV and Particle Image Velocimetry (PIV) techniques.[8] They proved that velocity measurements in flows with high turbulence intensities can be performed with high accuracy by optical methods. Great care must be used in taking measurements close to solid walls where high noise levels are present due to the scattering of light on the walls. The results of the PIV and LDV velocity measurement techniques were compared and showed that good measurements can be obtained from both techniques. The conclusion of their study proved that the comparison between PIV and LDV does not provide alternative, but rather complementary information.

The ability to perform high resolution, non-intrusive measurements in supersonic flows, particularly in complex flowfields such as shockwave/boundary layer or vortex/boundary layer interactions continue to create acute challenges for LDV instrumentation. The signal processors have limitation, especially in the frequency ranges of high speed flows.

There are few publications that describe LDV applications to high speed flows. The majority of these papers address LDV applications to transonic flows or high speed jets. Most of the papers that address high speed flow boundary layers are assessment tests or comparisons between hot-wire techniques and LDV. The comparisons examine only one or two characteristics of turbulence. This study describes a broad range of topics in turbulence including; mean velocities, turbulence intensities, Reynolds stress, autocorrelation and the energy spectra. To the best of our knowledge, there are no publications that address all of these characteristics of turbulence in such detail as we will attempt, in one paper.

Apparatus

Wind Tunnel Facilities

The boundary layer profile was obtained in the University of Central Florida's supersonic wind tunnel. The wind is a "blow down" type with a maximum Mach number of 5.0 and test section dimensions of 4 in x 4 in. The blow down duration at M = 2.5 is approximately 30 seconds.

Laser Doppler Velocimeter (LDV)

The turbulence profiles were obtained by a two dimensional LDV designed by Thermal Systems Incorporated (TSI). The light source is a Spectra Physics Model 2020 Argon Laser (six watt) operating in multi-line mode. The LDV was set up in off-axis forward scatter mode. The transmitting optics consist of an 1100 mm. lens and a beam spacing of 100 mm. The receiving optics consist of a 250 mm. lens to allow for a large solid angle of scattered light to be collected and were tilted upwards at 3 degrees (for alignment purposes).

The return Doppler signal was processed by two model 1990C (TSI) signal processors operating in coincidence mode. The processors were linked to a 40 Mhz. 386 computer via direct memory access (DMA) using a 6260 data acquisition card (TSI). The data was processed using FIND (TSI) software developed specifically for LDV.

Verification

Overview

The LDV verification involves a three stage process of verification before the boundary layer profile was obtained; 1) rotating disk, 2) free turbulent jet and 3) supersonic freestream

velocities in a wind tunnel at various Mach numbers. In the verification process, many concepts such as frequency shifting, optical arrangements and flow seeding methods were tried and proven. This section focuses on the methods that were proven to work and how conclusions were made.

Rotating Disk

The first experiment determined the angular velocity of a rotating disk. The true angular velocity was determined to be 91 revolutions per minute (rpm) by a stroboscope. The LDV was set up in back scatter mode with frequency shifting optics (Bragg cells) installed for both velocity components (**x** and **y**) to be measured and the laser set at minimum power (~ 250 mw). The center of the disk was used as the center of the coordinate system. Different points on the face of the disk, including all four quadrants, were used for verification The reason all four quadrants of the disk were used, was to verify frequency shifting application to velocity reversal.

For this low speed, constant angular velocity application, the turbulence intensities (fluctuations) were very close to zero (as expected). The LDV measured negative velocities for the **u** component in quadrants I and II and negative velocities for the **v** component in quadrants II and III (see Figure 1). The maximum relative error in angular velocity between the LDV and stroboscope was determined to be ~4.0 %. The majority of this error is due to the difficulties in positioning the measurement volume (laser beam) at the exact center of the rotating disk. This verification established the coordinate system and proved that optical alignment and frequency shifting was properly applied and understood.

Free Turbulent Jet

The second verification experiment involves the velocity and Reynolds stress profiles of a free turbulent jet. A six jet atomizer provided the necessary tracer particles and was adapted to have an exit diameter of 5 mm. The velocity profile was taken through the cross section at 38 diameters (190 mm) downstream of the jet. The LDV was set up in backscatter mode and frequency shifting was used for both velocity components.

The collected data was processed using FIND software and compared to published data[9] ; the mean velocity components (**u** and **v**, figures 2 and 3) profiles compared well. Notice the scatter in the Reynolds stress data (figure 4). The scatter is also present in the boundary layer profile. The possible causes and implications are discussed later.

Supersonic Freestream Velocities

The final stage of the verification process involves verifying the supersonic freestream velocity inside the wind tunnel at Mach numbers of 2.0, 2.5 and 3.0. The system was initially set up in back scatter mode, but the signal to noise ratio (S/N) was not adequate. The configuration was changed to off-axis forward scatter mode. For the wind tunnel application, no frequency shifting was needed for the freestream or **u** component of velocity because no flow reversals were expected.

The flow conditions in the wind tunnel presented a problem for the coincidence window in the signal processors. The problem is that the frequency of the freestream (**u**) component is about 45 Mhz (500-600 m/s), but the cross stream component is on the order of 1 Mhz (less than 20 m/s). If the coincidence window is to be set at 10% of the transient time through the

measurement volume, then the cross component signal will not have enough time to cross the amount of fringe required to satisfy the processor timer criteria and particle validation will be almost impossible. The result is an extremely low data rate and almost zero data validation.

The solution is to apply a frequency shift in the cross component and leave out the downmixing. The Bragg cell shifts the frequency by 40 Mhz and if no downmixing is used the cross component signal will have a frequency of 40 Mhz +/- the Doppler frequency caused by the particle moving in the cross component (**y**) direction. To account for the induced frequency shift, FIND software can be told that there is a 40 Mhz shift and the appropriate data processing will be performed by the software. This technique should only be used for extreme differences in Doppler frequencies, due to undesirable results in the turbulence intensity calculations for the shifted signal. The particular form of the equation used by the statistical analysis program causes the turbulence intensities to have unrealistically high values (over 100%) and should be disregarded.

The freestream velocities were verified by a pitot-static probe along with the known total pressure. The readings were taken during the same run of the wind tunnel to ensure identical flow conditions. The pitot-static probes determined the static pressure at the wall (p_{static}) of the wind tunnel and the total or stagnation pressure (p_2 behind a shock wave) in the freestream. The total pressure (p_1) of the flow is known by setting it at the control panel of the wind tunnel. The Mach number was verified by comparing the ratio of p_{static} and p_1 using tabulated isentropic flow relations and the ratio p_2 and p_1 using tabulated normal shock properties. The Mach numbers from the two different pitot-static measurements compared to within a 1.5% relative error.

Once the Mach number was determined, the static temperature was calculated from isentropic tables using a total temperature of 300 K and used in the Mach number-velocity relationship to determine the velocity of the flow:

$$Mn = \frac{V}{\sqrt{\gamma RT}}, \quad \text{or} \quad V = Mn\sqrt{\gamma RT} \qquad \textit{(Mach number - Velocity relation)} \ \textbf{(1)}$$

This velocity was compared to the velocity measured by the LDV. The Mach numbers used to verify the velocity were 2.19, 2.47 and 3.03. The results are as follows:

Mach 2.19:

p_{static} (wall)	3.79 psi	Static temperature	-120 C°
p_{01} (total)	40.0 psi	Total temperature	27 C°
p_{02} (behind shock)	22.6 psi	Velocity (pitot-probe)	542 m/s
		Velocity LDV	513 m/s
		Relative error	5.5 %

Mach 2.47:

p_{static} (wall)	3.33 psi	Static temperature	-138 C°
p_{01} (total)	54.0 psi	Total temperature	27 C°
p_{02} (behind shock)	28.0 psi	Velocity (pitot-probe)	574 m/s
		Velocity LDV	538 m/s
		Relative error	5.9 %

Mach 3.03:

p_{static} (wall)	2.22 psi	Static temperature	-166 C°
p_{01} (total)	85.0 psi	Total temperature	27 C°
p_{02} (behind shock)	26.6 psi	Velocity (pitot-probe)	621 m/s
		Velocity LDV	591 m/s
		Relative error	4.8 %

The corresponding relative errors are acceptable for high speed LDV measurements.[10] The pitot probe measurements tend to overpredict the LDV velocity by a fairly constant percentage. The majority of the error is in the estimate used for the total temperature of the flow. A 5% error is acceptable and relatively constant for all three velocity measurements. The free stream verification proved that the frequency shifting application for the **y** component was correctly applied as the data rates were increased by over 100%, compared to the measurements taken without the frequency shifting. In addition, the verification established that off-axis forward scatter mode configuration was properly aligned and applied.

Procedure

Near wall setup (0-2 mm)

The LDV system is setup in forward scatter mode with no frequency shifting for either the **x** or **y** component. The beam separation entering the transmitting optics is 50 mm and the focal length of the transmitting lens is 1100 mm. This corresponds to a fringe spacing of 11.32 micron for the green beam and 10.7 micron for the blue beam. The blue beam (488 nm) is oriented in the vertical plane and the green beam (514.5 nm) is oriented in the horizontal plane. The blue beam measures the cross component of velocity while the green beam measures the freestream component of velocity.

The receiving optics were setup at an off-axis position of approximately 7 degrees and a slight tilt of about 3 degrees toward the upper wall of the test section. The receiving lens has a focal length of 250 mm which provides a large (11.4°) solid return angle for the incoming Doppler

signal. Typically three to four measurements were made at each position so that the results where combined to produce an ensemble average.

Mid-Layer Setup

In the Mid-layer (3.0 mm to the freestream) it is necessary to use frequency shifting for the blue beam (cross component) with no down-mixing. This is due to the difference in the Doppler signal at the signal processors. If the signals have a large difference, the signal processors in coincidence mode will produce a very low data validation rate and the 25 second "blow down" duration will not allow enough time to collect the required data for statistics processing. The software must be configured so that the 40 Mhz frequency shift is accounted for in the statistical calculations.

Flow Seeder

Flow seeding is accomplished by injecting titanium-tetrachloride ($TiCl_4$) vapor into the stilling chamber ahead of the convergent-divergent nozzle of the wind tunnel. Once inside the stilling chamber of the wind tunnel, the vapor reacts with the moist air supplied from the pressure tank. This system was designed to utilize the moisture in the air supplied to wind tunnel. Particles are formed by a chemical reaction and there is no agglomeration or coagulation. The particle size is uniform and submicron. These two conditions are essential for LDV applications to high speed flows. The vapor reacts with the water present in the compressed air by the following chemical reaction:

$$TiCl_4 + 2H_2O = TiO_2 + 4HC \qquad (2)$$

The vapor is supplied from a pressure vessel containing liquid titanium-tetrachloride . Dry (compressed) air is blown through the chamber (pressure vessel) where the bottom of the chamber contains a small amount of liquid $TiCL_4$. The surface area of the liquid-vapor interface is 150 in^2. The vapor mixture is then injected into the stilling chamber of the wind tunnel (see Figure 5). The reaction with the moist air produces a consistent stream of titanium dioxide (TiO_2) particles of uniform size (~0.1 micron), with a high refractive index of 2.6 and density of 4200 (kg/m^3).[11]

In addition to the uniform particle size, the seed or tracer particles are monodispersive and free from coagulation. This is very important to ensure that the particles can follow the flow. If the particles coagulate, it produces a large clusters of particles that can seriously corrupt the data. Attempts were made using Al_2O_3 powder delivered from a fluidized bed, but it was apparent that coagulation and the presence of various descrete sizes or broad distributions of particle sizes existed in the flow. This produces multiple peaked or smeared histograms and can be observed in the real time histogram. The particle density is controlled by adjusting the differential pressure between the total pressure in the stilling chamber of the wind tunnel and the pressure of the pressure vessel. Typically a differential pressure (Δp) of 12-15 psi was used, but the value depends on several factors such as humidity, position in the boundary layer, and amount of liquid titanium-tetrachloride in the chamber (pressure vessel).

Results and Discussion

Overview

This section presents the results of the velocity, turbulence intensity and Reynolds stress profiles. Each measurement made by the LDV in the boundary layer is an ensemble average of 180-1600 signals (samples/measurement) validated by the signal processors as seed particles pass through the measurement volume. The results of the average are simultaneous, two dimensional measurements of the instantaneous velocity. At each point in the boundary layer, three or four measurements were taken and the results averaged to produce the profiles.

For validation measurements, the samples per measurement were *at least* 2024. However, difficulty in providing enough seed particles in the boundary layer along with a short "blow down" duration (25-30 seconds) in the wind tunnel resulted in low data rates and ultimately fewer samples per measurement. The low speed applications had data rates of 250-400 signals per second. The time required to gather 2024 valid signals was about ten seconds. For the supersonic freestream measurements, the data rates were 125-250 signals per second, requiring a minimum of 10-15 seconds to assemble 2024 signals. In the boundary layer, the data rates seldom exceeded 75 per second, resulting in less than 2024 valid signals gathered during any one measurement.

The statistics of turbulence is sensitive to the number of data points collected. Statistical methods are more reliable if a large number of data is taken during sampling. The effect of low data rates causes problems in the calculations that show up in different measurements. The problems of low data validation rates are addressed as they apply to each statistic.

Velocity Profiles

The velocity, turbulence intensity and Reynolds stress profiles were taken along the upper wall of the test section, where the approximate boundary layer thickness is five mm. The wall of the test section was roughened to produce a thick boundary layer due to the relatively large measurement volume diameter (~1mm). A freestream Mach number of 2.47 was determined by pitot-static probe measurements and the total pressure setting of the wind tunnel.

u Component (longitudinal)

The mean velocity profile shown in Figure 6 displays the typical profile expected in a turbulent boundary layer along a wall. The figure displays the maximum velocity gradients in the region from $0.0 < \frac{y}{\delta} < 0.7$. These gradients are as large as 150 m/s per mm. This is expected in high speed flows and can reach much higher values along the wall closer to the nozzle or in a thinner boundary layer. In the near wall region, large Naturally Occurring Particles (NOP) in the form of ice or frozen water vapor, originating from the freestream were hurled against the wall, making signal processing difficult and requiring many iterations through the signal processor optimization.

Figure 6 shows two profiles in non-dimensional form to account for variations in test conditions. The agreement between the measured data and published profiles is acceptable, with a maximum relative error of 6.7 % and an average of 2.4 %. For the region $\frac{y}{\delta} \sim 0.4$, there is some evidence of velocity bias. The rate at which seed particles pass through the measurement volume is directly proportional to the fluid velocity. Velocity bias is generated by the velocity variations across the measurement volume that are caused by velocity gradients present in the flow. In the high velocity region, more particles pass through the measurement volume than in the low

velocity region. The result is velocity histograms skewed towards the higher values (Figure 7). As a comparison, Figure 8 shows a typical velocity histogram with good signal to noise ratio and no evidence of velocity bias. The smoothness of the curve and lack of scatter in the data shown in Figure 6 demonstrate the effectiveness in application of seeding and proper experimental technique.

v Component (normal component)

The **v** component of mean velocity displays the largest velocity gradients between $0.6 < \frac{y}{\delta} < 1.0$ which is the region of the boundary layer and the freestream interface. As the vortex lines are created against the wall, they continue to grow until they reach the boundary layer and the freestream interface. At the boundary layer interface region, the eddies are moving away from the wall at the maximum velocity. The general movement of eddies away from the wall produces problems in delivering seed particles in the boundary layer. It is a common observation that the walls of the wind tunnel become coated with a film of particles used for seeding. This indicates that the flow inside the viscous sublayer is such that a particle which enters the sublayer has a very low probability of leaving.[12] A particle entering the viscous sublayer becomes caught up in the motions of the longitudinal vortices, and ends up on the walls. Consequently, a fluid element coming from the wall is less likely to carry particles than a fluid element moving towards the wall. As a result, this region is susceptible to large errors in measurement due to the problems with seeding.[13] In addition, the presence of large NOP's in the boundary layer will produce a Doppler signal with a large signal to noise ratio. The NOP's do not follow the flow through velocity gradients present in the boundary layer due to their size and mass. It is essential that their signal

is filtered out so that only the signal produced by the smaller seed particles are validated for velocity information.

For the region $\frac{y}{\delta} = 0.0$ to $\frac{y}{\delta} \sim 0.4$, no frequency shifting was used. However, in the region of $\frac{y}{\delta} \sim 0.5$ and above, frequency shifting (using a Bragg cell) with out downmixing, was used for the **v** component. Downmixing removes the frequency shift induced by the Bragg cell. This application of frequency shifting was used due to the large difference in Doppler frequencies between the two components in the outer region of the boundary layer. A large difference in Doppler frequencies presents problems for simultaneous two dimensional velocity measurements. The coincidence window allows the signal processors to measure the **x** and **y** velocity components of the same particle. The proper coincidence window setting is about 10% of the particle transient time through the measurement volume. If there is a large difference in velocity between the **x** and **y** components, the particle may not have time to cross enough fringes in one direction to satisfy processor criteria and particle validation will be impossible.

The solution is to apply frequency shifting to the low velocity component and remove downmixing. The Bragg cell shifts the frequency of the laser beam by 40 Mhz and if no downmixing is used the shifted signal will come into the signal processors at 40 Mhz +/- the Doppler frequency. Using this technique, the data validation rates are increased and more samples can be taken in a shorter time duration. Figure 9 shows good continuity between the region of $0.4 < \frac{y}{\delta} < 0.5$, demonstrating proper use of this frequency shifting technique.

Turbulence Intensities

The longitudinal fluctuations (**u'**) are slightly larger in magnitude than the lateral fluctuations (**v'**) as shown in Figures 10 and 11. This is because the shear production of

turbulence initially feeds the energy into the **u**-component and then the energy is distributed into the **v**-component.[14] At the near wall, the turbulence intensity initially rises as the wall is approached.[2] However, due to limited optical access, the LDV cannot reach the inner wall region. Therefore, **u'** and **v'** could not be measured inside of $\frac{y}{\delta} = 0.1$. The turbulence intensities of the **u** component (Figure 10) show a sharp drop with increased distance away from the wall. This profile is in good agreement with published hot-wire data[4].

The **v** component (Figure 11) displays a maximum intensity close to the wall, but does not drop off as quickly as the u component. This trend also agrees with published hot-wire data.[2,9] The effects of using frequency shifting is more obvious for this statistic than the mean velocity. The profile shows a steady and consistent drop off as the distance from the wall increases. However, at the point where the frequency shifting was imposed ($0.5 < \frac{y}{\delta} < 0.6$), the profile has a slight increase in turbulence before dropping off.

The comparison of LDV data to published hot-wire data verifies that proper seed delivery in the boundary layer was accomplished for the turbulence intensity profiles and proper experimental technique was used. Even though the LDV does not take data at even time intervals, it appears that sampling at unequal time intervals gives satisfactory turbulence intensity values even at low to moderate data rates.

Reynolds Stress

The Reynolds stress is the most difficult statistic to determine using an LDV in high speed flows. The effect of the large rate of strain on the seed particles in the boundary layer is not clear and remains an open question. Some researchers believe that in regions of large strain the seed or tracer particles simply do not follow the flow properly[13]. Others believe that the anomalies in

Reynolds stress calculations arises because the scattering particle number density is very strongly correlated with the instantaneous stress and not as a result of any local failure of the particles to track the flow.[12]

For this study, the Reynolds stress profile (Figure 12) is scattered. However, the values are negative as expected. The scatter is most likely caused by the numerical method used in the software to calculate the Reynolds stress from raw data. The Reynolds stress is defined as:

$$\overline{uv} - \overline{u} \times \overline{v} \qquad (3)$$

There is a certain amount of error associated with each statistic, when two separate statistics are multiplied together (namely **u** and **v**) to obtain the Reynolds stress, the error associated with the calculation is further multiplied.

To minimize the error associated with the Reynolds stress calculations in high speed flows using an LDV, it is necessary to have a large amount (above 3000 points) of data per measurement . Statistical calculations of higher moments are sensitive and can result in scattered data if there are not enough data points.[10] The result of the data rate limitations and the corresponding error are scattered data for the Reynolds stress calculations through out the boundary layer. The line drawn through the data is an attempt to describe how the Reynolds stress profile should look through the boundary layer.

The values of Reynolds stress are expected to be negative. Physically, when a small packet of fluid is moving, a loss of momentum (caused by a local instability) slows the fluid down resulting in an inflection point in the velocity profile. This causes the spanwise (longitudinal) vortex lines to stretch until they break producing small scale turbulence. This causes a positive

movement in the **y** direction and a resulting negative burst of motion in the **x** direction, creating a negative Reynolds stress. Likewise, if the opposite phenomena occurs (an initial negative **y** movement) a positive burst of motion is created in the **x** direction from the faster particle colliding into a slower particle. Either way a negative Reynolds stress is created.

Autocorrelation

The autocorrelation function can be used to determine the approximate size of the smallest eddies. The curvature at $\tau \sim 0$, as determined by the second derivative of the autocorrelation function represents an estimation of the size of the smallest eddy.[15] In general, the sharper the curvature, the smaller the size of the eddies. Figure 14 shows the autocorrelation function for the **u**-component and Figure 15 the **v**-component. If the second derivatives of these curves were taken, it is obvious that the curvature for the **v**-component would be much larger than the **u**-component, because a large radius corresponds to a small curvature. Therefore, the scale of turbulence (size of eddies) is smaller for the **v**-component (lateral) than for the **u**-component (longitudinal). This is expected in a boundary layer because $\mathbf{u} >> \mathbf{v}$. If $\mathbf{x} >> \delta$ in the boundary layer, the boundary layer assumption is satisfied (see figure 13).

$$\frac{x}{u} \approx \frac{\delta}{v} \qquad \textit{(boundary layer assumption)} \qquad (4)$$

Distance over velocity has the units of time. Therefore, the correlation time scale in the **x** direction is less than the correlation time scale in the **y** direction.

Energy Spectrum

All of the various sized eddies that make up turbulent motion have a certain kinetic energy. This is based on their vorticity or by the intensity of velocity fluctuations of corresponding frequency. The energy of turbulence is dissipated into heat by the cascade process. Large eddies or vortices are formed in the boundary layer. Their size is governed by the mean flow. The large vortices will break down into smaller and smaller vortices, whose velocity gradients are large enough for viscosity to play a significant role. Their kinetic energy is dissipated into heat through viscosity. The energy spectrum shown in Figure 16 demonstrates that the energy at a point is distributed over a wide range of frequencies confirming the cascade process. No eddies of size smaller than the Komolgorov scale (λ_g) can be found on the power spectrum because when λ_g is reached the kinetic energy is dissipated into heat.

The low end of the frequency range represents the largest eddies and the high frequency range represents the smallest eddies. Figure 16 demonstrates that the largest eddies are energy containing and the smallest eddies energy dissipating. The largest eddies at the left end or low frequency end portion of the spectrum have a larger value of energy. The right end or high frequency region stops abruptly, meaning that there are no eddies smaller in size. By conservation of energy, the kinetic energy in the large vortices equals the dissipation rate in the smallest vortices. This is called "Komolgorov's Universal Equilibrium Theory of Small Scale Structures". The energy content is equal because there are many more small scale vortices than large vortices, although each smaller eddy contains less kinetic energy. In the region between the high and low frequencies (inertial subrange), the slope of the energy spectrum (figure 16) obeys Komologorov's $-\frac{5}{3}$ law. The role of the inertial subrange is to transfer kinetic energy from large eddies to smaller eddies, and its range increases with Reynolds number.[16]

Boundary Layer Analysis

In the outer region of the boundary layer there is a supply of kinetic energy from the freestream flow or upper parts of the boundary layer where inertial transfer of energy is the dominating factor. Turbulence in this range is statistically independent of the energy containing eddies and the range of strong dissipation (viscous sublayer). This energy is converted through work done by the turbulent shear stresses into production of turbulent energy in the inner part of the boundary layer. In the wall region of the boundary layer, most of the turbulence is converted directly into heat by turbulent dissipation. Part of this energy is transported by turbulent diffusion toward the outer region of the boundary layer.

As an overview to the process, there is an influx toward the wall of energy originating from the mean flow, converted into turbulent energy, which is in part directly dissipated but put back in part by turbulence into the outer region.[16]

Conclusions

Laser Doppler Velocimetry was used to measure $\bar{u}$, $\bar{v}$, u', v' (rms values), autocorrelation and energy spectra. These results compare well with published data. However, the measurement technique does not provide accurate results for the Reynolds stress.

Al_2O_3 particles, used for flow seeding by many researchers who use LDV techniques, did not work well for our applications due to agglomeration. High humidity of Florida air caused the particles to cluster together, resulting in particles that were too large and were dispersed in several different sizes. A TiO_2 seeder was developed and worked extremely well for the humid conditions. The chemical reaction of $TiCl_4 + H_2O$ resulted in the formation of TiO_2 particles inside the wind tunnel. These particles are uniform in size (~0.1 micron) and well suited for high speed LDV applications.

The frequency shifting technique used to reduce the difference in frequency between the Doppler signals in the boundary layer increased the data rate by over 100%. This is a positive step in overcoming the signal processor limitations associated with LDV applications in high speed flow boundary layers.

Finally, this study has contributed to an experimental data base of existing limited collections of high speed flow velocity and turbulence data. This contribution is unique because it covers a broad range of turbulence characteristics. This class of information is currently needed for CFD code verification in high speed flows to produce design caliber computational codes for aerodynamic applications. In addition, the study describes the methodology involved in the setup, application and troubleshooting of Laser Doppler Velocimetry flow measurements.

References

1. Malik, Mujeeb R.; "Prediction and Control of Transition in Supersonic and Hypersonic Boundary Layers", AIAA Journal, v 27, pp 1487-93 November 1993

2. Donovan, J. F. and Spina, E. F.; " An Improved Analysis Method for Cross-Wire Signals Obtained in Supersonic Flow", Proceedings from Spring meeting of the Fluids Engineering Division, ASME, June 4-7, Ontario, Canada

3. Bertuccioli, L. and Degrez, G.; "Application Of LDV to Supersonic Laminar Boundary Layer Flows", AIAA Paper 93-3069, July 1993

4. Donovan, J. F. and Spina, E. F.; " An Improved Analysis Method for Cross-Wire Signals Obtained in Supersonic Flow", Proceedings from Spring meeting of the Fluids Engineering Division, ASME, June 4-7, Ontario, Canada

5. Knight, Doyal., Hortsman, C. C., Bogdonoff, S.; "Structure of Supersonic Turbulent Flow Past a Swept Compression Corner", AIAA Journal, v 30, pp890-6, April 1992

6. Hall, R. M., Obarg, C. J., Carraway.C.L.; "Comparison of Boundary Layer Transition Measurements Techniques at Supersonic Mach Numbers", AIAA Journal, v29, pp 865-71, June 1991

7. De Campos, J. A., Falcao, C.; "Laser Doppler Measurements on Tip Vortices in Non-cavitatind and Cavitating Conditions", ASME Fluids Engineering Division, V 135, p63-68

8. Romano, G. P.; "PIV and LDV Velocity Measurements Near Walls and in the Wake of a Delta Wing", Optical Engineering, v16, No. 4-5, p293-309, 1992

9. Schetz, Joseph A.; Boundary Layer Analysis, Prentice-Hall, 1993

10. Private Communication with Greg Reynolds, TSI Application Engineer, 1993-1994

11. Private Communication with Richard Gould, University of North Carolina, September 1993.

12. Dimotakis, Paul E., Lang, Daniel B., Collins, Donald J.; "Laser Doppler Velocity Measurements in Subsonic, Transonic and Supersonic Turbulent Boundary Layers", AEDC-TR-79-49, 1979

13. Private Communication with Eric Spina, Syracuse University, New York, June 1994

14. Kundu, Pijush K,; Fluid Mechanics , Acedemic Press 1990

15. Cebeci, Tuncer., Smith, A. M. O.; Analysis of Turbulent Boundary Layers, Academic Press 1974.

16. Hinze, J. O.; Turbulence, McGraw-Hill, 1975.

APPENDIX 1

Figures

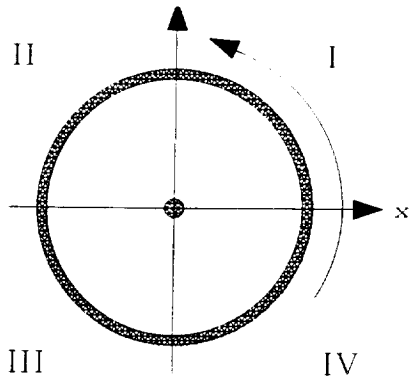

Figure 1 Coordinate System of Disk

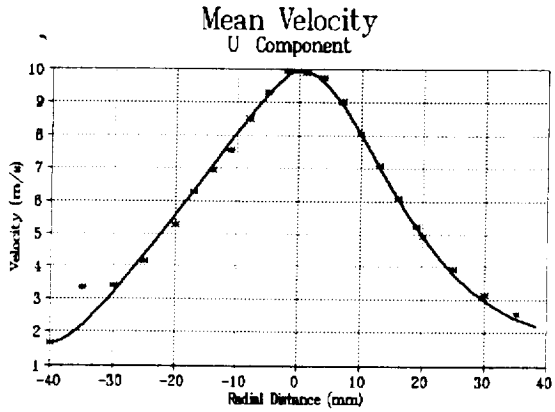

Figure 2 Free Turbulent Jet (u Component)

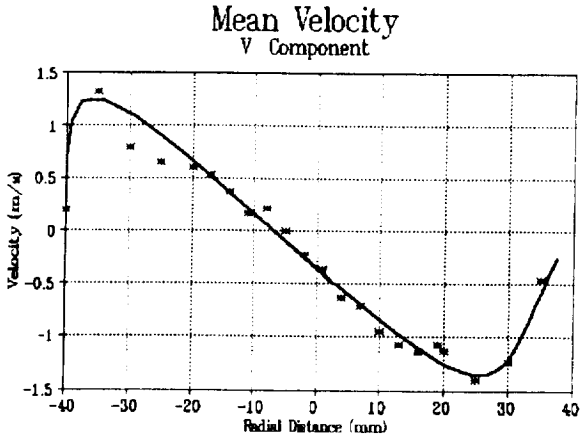

Figure 3 Free Turbulent Jet (v Component)

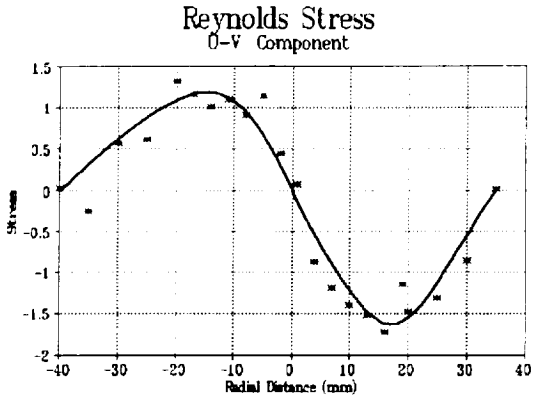

Figure 4 Free Turbulent Jet (Reynolds Stress)

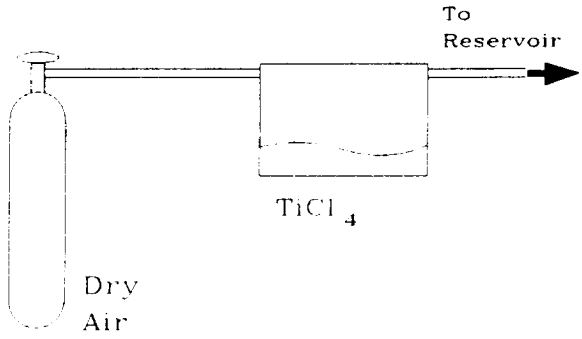

Figure 5 Flow Seeding Delivery System

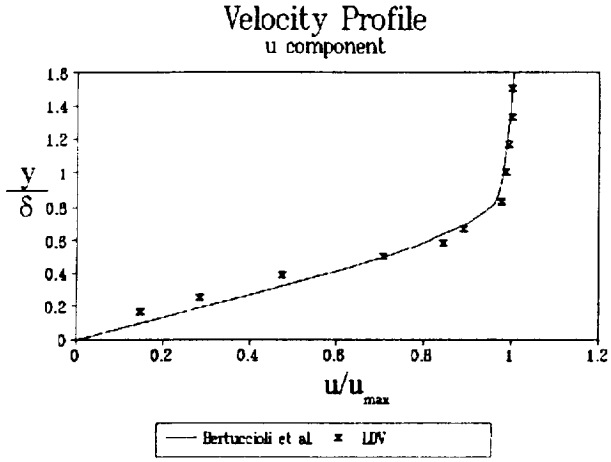

Figure 6 Boundary Layer Profile (u Component)

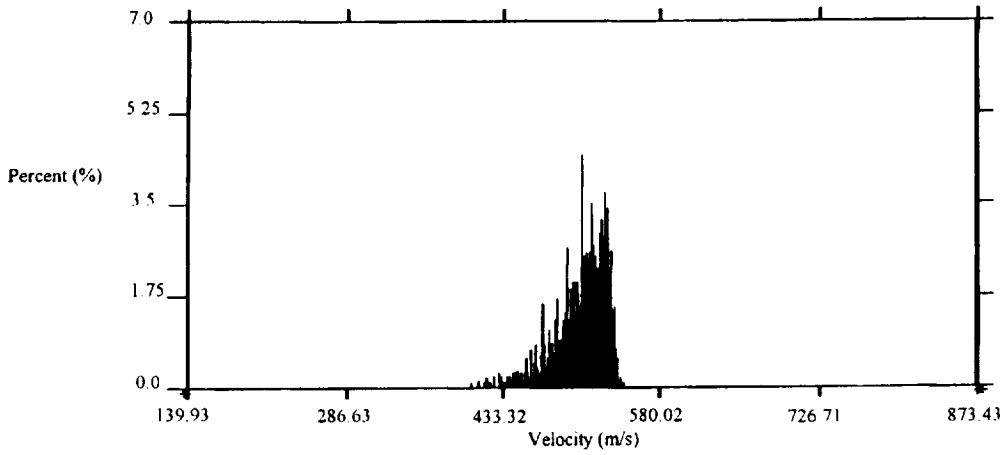

Figure 7 Skewed Histogram

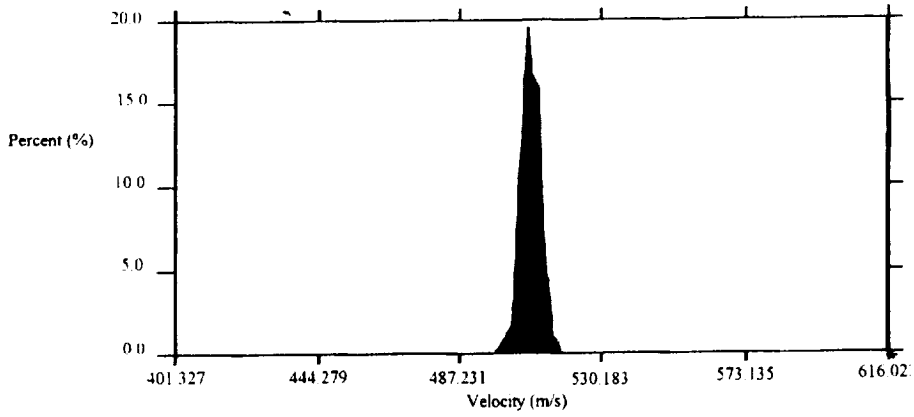

Figure 8 Velocity Histogram

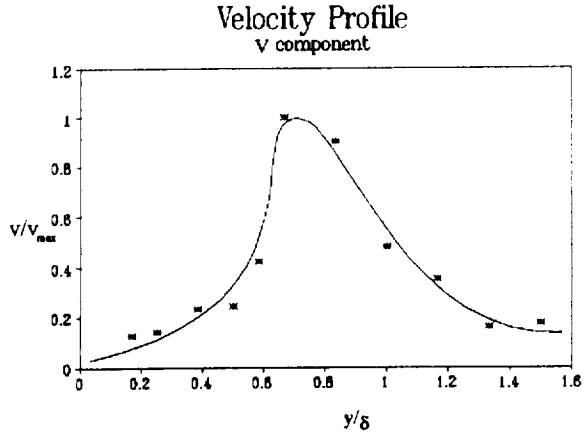

Figure 9 Boundary Layer Profile (v Component)

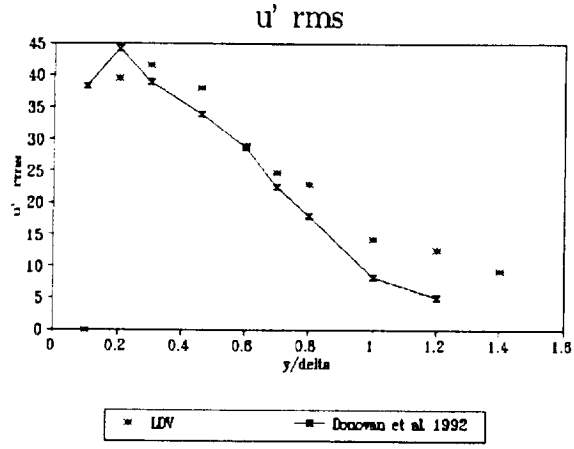

Figure 10 Turbulence Intensity (u Component)

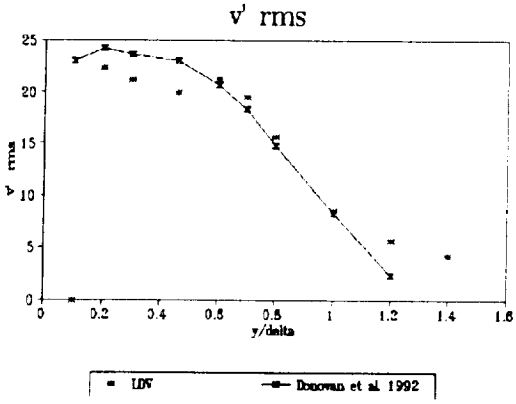

Figure 11 Turbulence Intensity (v Component)

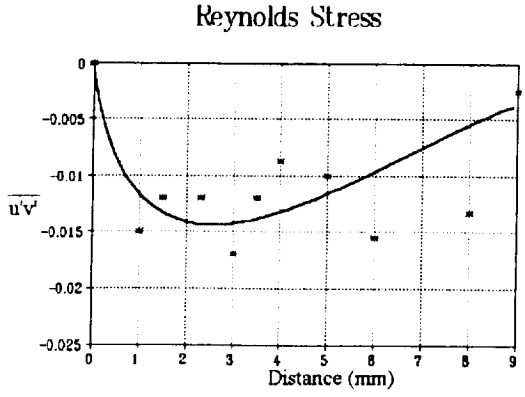

Figure 12 Boundary Layer Schematic

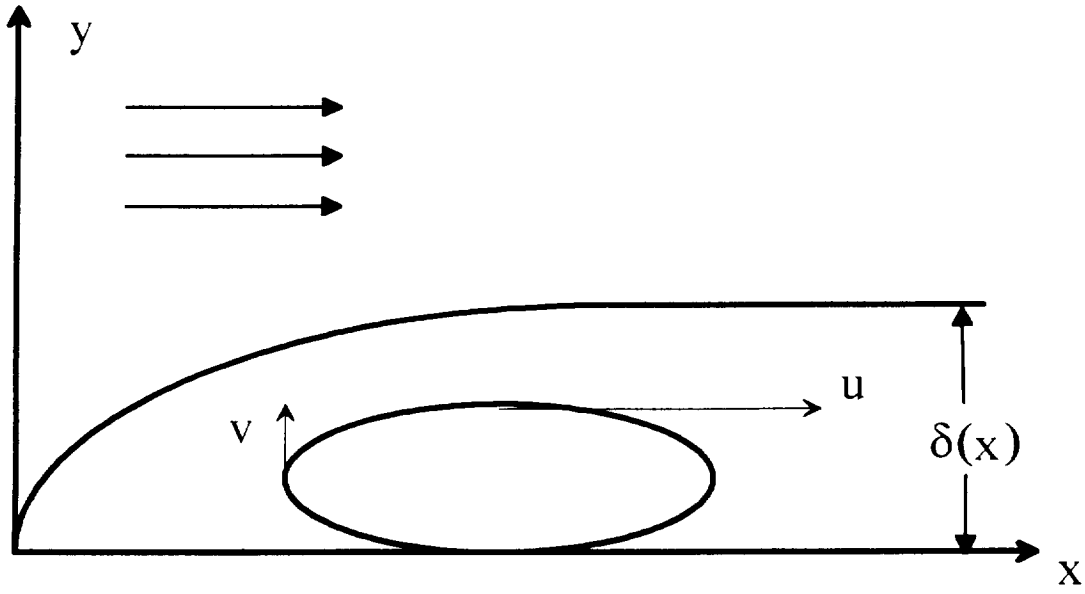

Figure 13 Boundary Layer Schematic

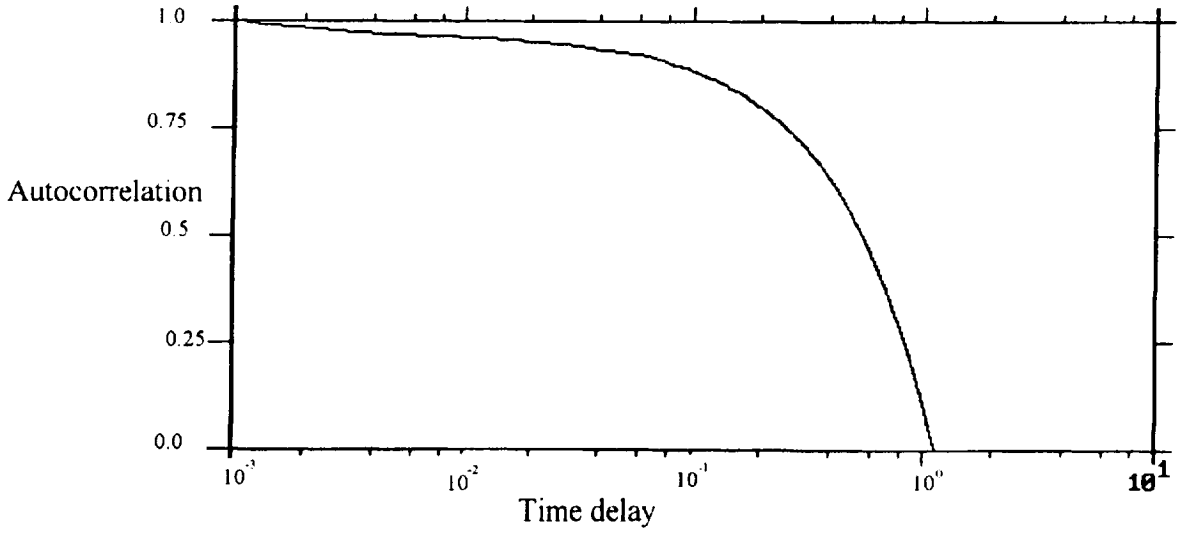

Figure 14 Longitudinal Autocorrelation Function

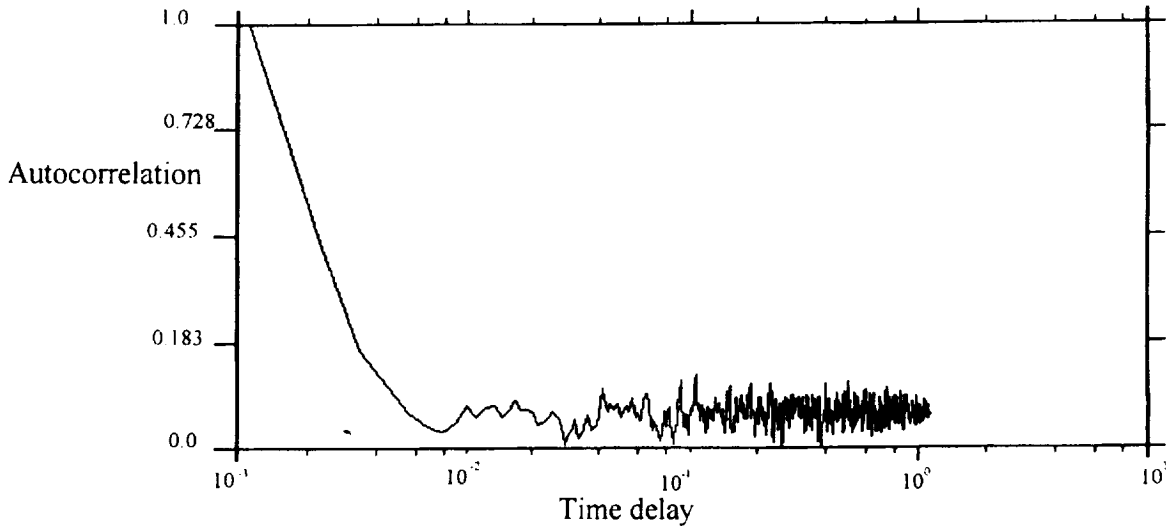

Figure 15 Lateral Autocorrelation Function

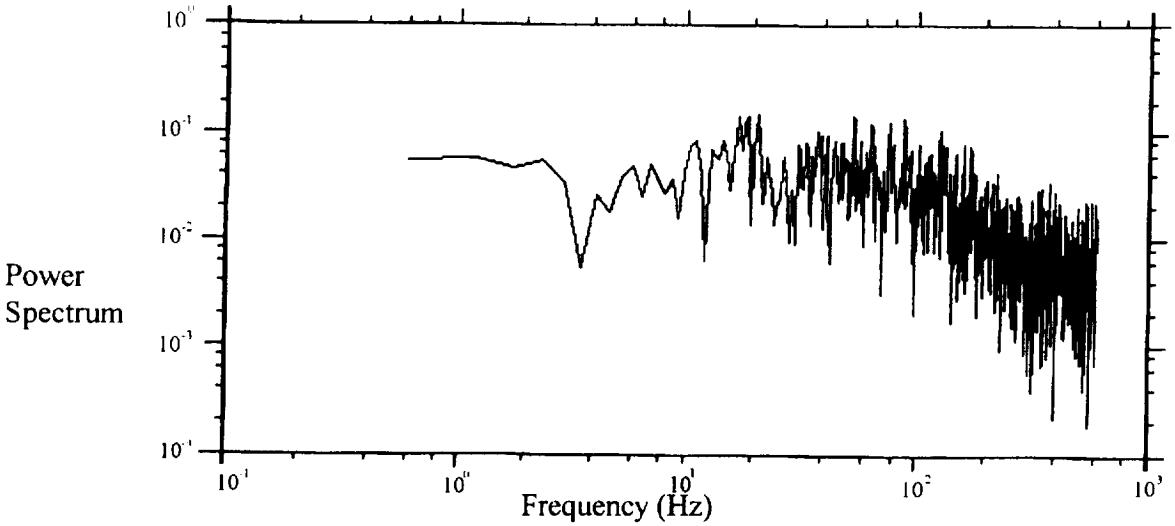

Figure 16 Energy Spectra